Sensors and Materials, Vol. 34, No. 4 (2022) 1549–1558
MYU Tokyo

S & M 2909

Strain Monitoring of Main Beam of Cable-stayed Bridge Based on Weak Grating Array

Zhiang Liu,[1,2*] Jianxin Zheng,[1,2] Hao Zhu,[1,2] Zichao Wang,[1,2] and Huadong Yang[1,2]

[1]CCCC Second Harbor Engineering Company Ltd., Wuhan, Hubei 430040, China
[2]CCCC Highway Bridge National Engineering Research Centre Co. Ltd., Beijing 100032, China

(Received February 7, 2022; accepted March 15, 2022)

Keywords: weak grating array, cable-stayed bridge, main beam, strain monitoring

To study the strain monitoring performance of weak grating array technology in the main beam of a cable-stayed bridge, the strain measurement of the steel truss main beam is carried out for the Yangtze River Bridge of Baijusi in Chongqing. Wavelength division multiplexing (WDM) and time division multiplexing (TDM) techniques were used for signal demodulation. Along the steel truss main beam, a strain measurement fiber with a grating spacing of 0.5 m and a temperature compensation fiber with a grating spacing of 2 m were laid in the measurement sections of the upper and lower chords. The strain state of the main beam during the bridge construction was then measured continuously over a 48-hour period. The results show that the weak grating array technology can collect data in real time in accordance with the predetermined acquisition frequency, and has good performance in the distributed strain monitoring of the main beam of the cable-stayed bridge. By combining these results with the temperature compensation scheme and monitoring design described in this paper, the influence of the construction state on the force of the main beam can be faithfully reflected. The results of the study provide a scientific reference for the use of weak grating array technology for the health monitoring of cable-stayed bridge structures.

1. Introduction

China has made remarkable achievements in bridge construction, and a large number of large-span bridges have been built.(1) Among them, cable-stayed bridges include Changtai Yangtze River Bridge, Chongqing Baijusi Yangtze River Bridge, and Sutong Bridge. In their construction and operation, the main beam of the steel structure supports most of the weight of the upper structure of the bridge, and it is of great significance to monitor the strain state of the main beam, the suspension beam, and the cable during the construction period to analyze the stress of the bridge structure and assess the health of the bridge.

Because of the characteristics of the main beam of a bridge with a large span and long construction and operation duration, sensors used for monitoring must be able to monitor many measurement parameters and to have a long service life. Conventional transducers such as strain

*Corresponding author: e-mail: kawhigo@foxmail.com
https://doi.org/10.18494/SAM3859

ISSN 0914-4935

gauges and displacement gauges do not meet these needs. Weak grating array technology based on a fiber grating can use single or multiple optical fibers to achieve long-distance continuous measurement, can accurately give changes in information such as strain, temperature, and vibration at a certain point on the optical fiber, and can realize large-scale distributed monitoring. Sartiano and Sales conducted quasi-distributed temperature sensing and single-point vibration sensing studies using weak grating arrays, and proposed an experimental method for sensing mechanical vibrations with frequencies as high as 245 kHz and strain resolution as small as 1.2 με.[2] Zhang *et al*. proposed a high-speed and high-multiplex distributed temperature sensor network based on a weakly reflective fiber grating and engraved three high-reflectance and low-bandwidth fiber Bragg gratings on a single fiber, realizing a temperature measurement error of ±0.5 °C and a spatial resolution of 10 m.[3] Li *et al.* proposed an optical fiber sensing system based on two weak fiber Bragg gratings (WFBGs) for simultaneous sensing of temperature and vibration. The temperature measurement range in their experiment was 20 to 100 °C and the measurement error was less than 0.1 °C, enabling the vibration signal to be accurately recovered at different temperatures.[4] Jiang and co-workers used weak grating array technology to monitor civilian infrastructure.[5,6] Luo *et al*. conducted studies on the preparation of ultraweak Bragg gratings.[7,8] Xin *et al*. performed ground intrusion event identification on subway tunnels using weak grating array technology.[9] The transfer of strain between the optical fiber and the structure under test is the key to the measurement accuracy, and this aspect has also been studied.[10–12]

From the above research, it can be seen that the weak grating array technology has achieved certain key results that verify the feasibility and economy of the technology for engineering applications, and has the characteristics of high density, high precision, and distributed measurement. However, there have been few practical applications of this technology to bridges, and a traditional point sensor is still used for the strain monitoring of the main beam of a bridge. In this paper, weak grating array technology is applied to the strain measurement of the main beam during the construction of the Yangtze River Bridge of Baijusi in Chongqing, and the strain state of the main beam during the construction of the bridge is continuously monitored for 48 h.

2. Basic Principles

2.1 Principle of weak grating array

A fiber Bragg grating (FBG) is used in a UV light exposure technique that produces a periodic refractive index distribution of the fiber core with photosensitivity, resulting in wavelength selectivity. That is, light of a specific wavelength is reflected and light of other wavelengths can pass through the FBG normally, making the FBG equivalent to a narrowband reflective filter, as shown in Fig. 1. The grating reflection equation is

$$\lambda = 2n_{eff}\Lambda, \tag{1}$$

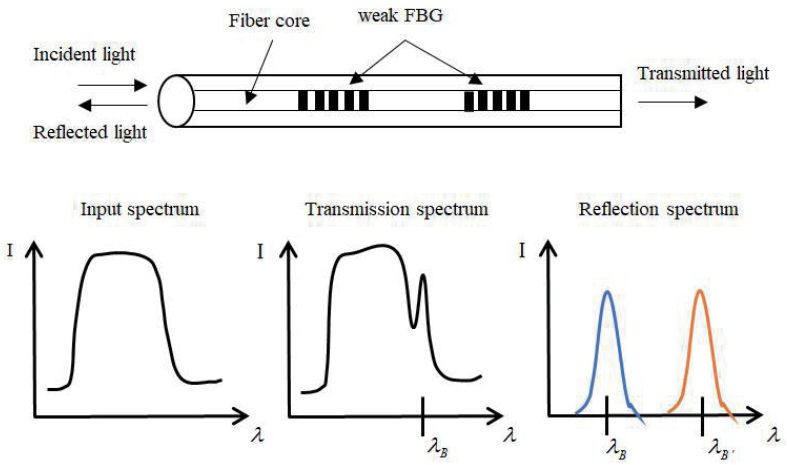

Fig. 1. (Color online) Sensing principle of weak grating array.

where λ is the FBG center wavelength, n_{eff} is the effective refractive index of fiber core, and Λ is the grating period.

When considering both strain and temperature variations, the center wavelength change of the FBG can be expressed as

$$\Delta\lambda = K_\varepsilon \varepsilon + K_T \Delta T, \tag{2}$$

where K_ε is the sensitivity coefficient between the change in the central wavelength and the axial strain of the optical fiber, and K_T is the sensitivity coefficient of the FBG in temperature sensing.

As can be seen from Eq. (1), if n_{eff} or Λ changes, the FBG center wavelength will drift. By measuring the drift of the FBG center wavelength, changes in the signal under test outside, such as strain and temperature changes, can be determined.

A weak grating array is based on the principle of FBG sensing. In such an array, a large number of ultraweak gratings (microstructures) with reflectivity of less than 0.1% are inscribed on an optical fiber, as shown in Fig. 1. By analyzing optical wavelength information on weak grating arrays, the sensing of external environmental changes can be achieved in a distributed manner. Through wavelength division multiplexing (WDM) and time division multiplexing (TDM) technologies, the number of grating sensors can be significantly increased, which in turn increases the sensing distance and enables high-resolution and long-range distributed sensing networks.

2.2 Principle of system operation and temperature compensation

The deformation coupling of a sensing fiber used to monitor a structure under test determines the validity of the measurement results. The weak grating array optical fiber by the surface layout method is pasted to the surface of the structure using a binder, and the binder is cured to

form an adhesive layer. Then strain is transferred via the adhesive layer, whose cross section is shown in Fig. 2.[13]

The strain transfer process between the WFBG and the structure under test is assumed to be as follows.

1) The materials have linear elasticity, and the strain received by the optical fiber originates only from the strain generated by the structure to be measured in its axial direction. The strain is transmitted through the bonding layer, and the optical fiber is not directly stressed.
2) The optical fiber is closely connected to the bond layer and the structure to be measured, and there is no relative displacement.

In this study, we use the reference fiber method for temperature compensation; it is the most commonly used method to solve the cross-sensitivity problem of distributed fiber optic sensors. This method has the advantages of simplicity and reliability. The principle of this method is to arrange the temperature compensation fiber in parallel next to the strain measurement fiber, as shown in Fig. 3, so that the temperature compensation fiber is in a state of free relaxation without strain and is only sensitive to changes in temperature, and the strain measurement fiber is installed on the structure to be measured by a comprehensive paste or fixed point paste method, so that it is sensitive to temperature and strain. The temperature information of the structure to be measured is obtained using the temperature compensation fiber. Then, in accordance with Eq. (2), this part of the information can be eliminated, so as to obtain the accurate strain information in the structure to be measured.

3. Engineering Application

3.1 Project overview

To verify the feasibility and test the accuracy of strain measurement of the main beam of a bridge using a weak grating array, a strain test was carried out at the Yangtze River Bridge of Baijusi in Chongqing. This bridge, which is still under construction, will connect the Chenjiage

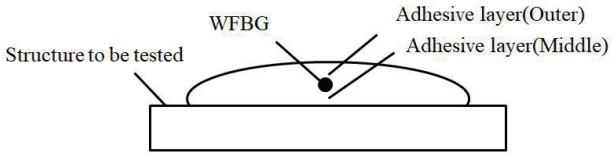

Fig. 2. Cross section of WFBG layout

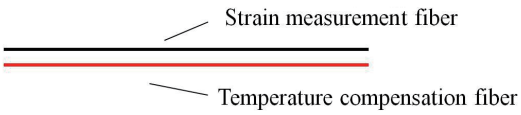

Fig. 3. (Color online) Positions of fibers in reference fiber method.

Interchange in Dadukou District and the Taiyanggang Interchange of The Ring Expressway in Banan District. The main bridge, shown in Fig. 4, is 1384 m long (its span is 107 + 255 + 660 + 255 + 107 m). The main beam steel truss adopts two triangular trusses, a center distance of the main truss of 18 m (equal spacing arrangement), a truss height of 12.606 m, and an internodal length of 15 m. The steel truss beam section adopts an inverted trapezoidal shape, a total bridge deck width on the standard section of 38 m, and a total lower bridge deck width of 19.2 m. The main truss is composed of an upper winding rod, a lower stringer, an abdominal rod, an edge stringer, and an inclined rod.

3.2 Monitoring scheme design

For the special environment of the strain measurement of the main beam of the bridge, we specially customized the sensing fiber based on the weak grating array with a fiber diameter of 0.9 mm (with protective sleeve) and gate point reflectance of 0.01%. The specific parameters are shown in Table 1. The strain fiber accommodates the three wavelengths of 1531, 1543, and 1555 nm in the grating point spacing arrangement for demodulation using wavelength division multiplexing and time division multiplexing technology. The temperature compensation fiber is composed of 1531 nm wavelength grating points.

A measurement fiber is arranged on the upper and lower chords of the main beam, as shown in Fig. 5. The position of the measurement fiber is upstream of Pier 7 (P7), between the lower chord B38 and B44 (a total length of 90 m) and the upper chord J12# cable–J15# cable (a total length of 45 m). The optical fiber is alongside the following path: lower chord strain measurement fiber–lower chord temperature compensation fiber–connection jumper–upper chord temperature compensation fiber–upper chord strain measurement fiber. On the basis of laboratory and on-site construction experience, we selected the surface paste method for laying out the optical fiber.

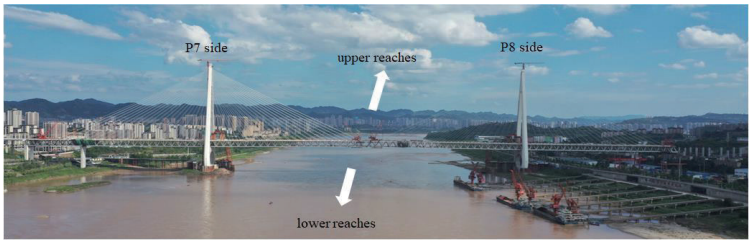

Fig. 4. (Color online) Yangtze River Bridge of Baijusi in Chongqing.

Table 1
Optical fiber parameters.

Number	Name	Measuring point density (m)	Wavelength (nm)
1	Lower chord strain fiber	0.5	1531, 1543, 1555
2	Lower chord temperature fiber	2	1531
3	Upper chord strain fiber	0.5	1531, 1543, 1555
4	Upper chord temperature fiber	2	1531

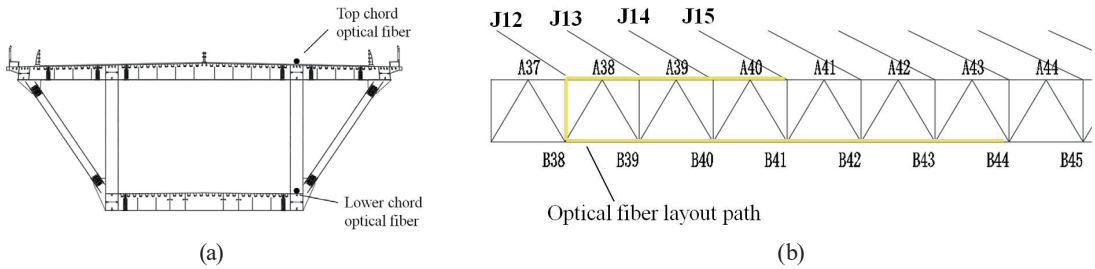

Fig. 5. (Color online) Optical fiber layout on the main beam: (a) cross section and (b) front view.

During the laying of the fiber and the filling of glue, the sensing fiber is always in a straightened state as shown in Fig. 6. The specific layout method is optical fiber pre-tensioning after the use of 502 glue at the fixed point on the main beam, where the pre-tensioning tension is controlled within the appropriate range. After the glue is dried, the adhesive (AB glue) is applied along the length of the optical fiber, and then, a glass fiber cloth is attached to protect the optical fiber. After the glue has cured, the strain is transmitted via the inner layer of the adhesive layer to form a composite structure: substrate–adhesive layer–optical fiber–adhesive layer. In addition, the temperature-compensation fiber is laid in a stress-free state next to the strain fiber so that it remains in a relaxed state and is only affected by the temperature. The strain and temperature compensation fibers are spliced at the endpoint, and the upper and lower chord fibers are connected with 50-m-long armored jumpers to form a path, which is connected to the demodulation equipment through the lower chord fiber. After the layout is completed, the welding section and bending section are protected by a plastic box to avoid any damage to the optical fiber that would otherwise affect the subsequent test results.

The fiber optic layout was completed on July 18, 2021, and the commissioning ended on July 19, 2021, after which the measurement system operated stably. From 11:02 on July 20, 2021, the acquisition frequency was 30 s/time, and it ended at 11:02 on July 22, 2021, a total time of 48 h with 5761 data collections.

3.3 Analysis of monitoring results

After the test, each raw wavelength datum was plotted with a time interval of 1 h, giving a total of 48 data values, as shown in Fig. 7. By referring to the factory calibration results of the prestapled weak grating array fiber, the weak grating points with abnormal central wavelengths were corrected manually.

As shown in Fig. 8, the first data value collected at 11:02 on July 20, 2021 was selected as the initial value, and the data were subsequently collected at intervals of one hour. By subtracting the initial value from each subsequently obtained value, the change in the weak grating wavelength of the main beam during the measurement period can be determined. Along the longitudinal length of the main beam, when the main beam is stretched, the fiber wavelength becomes longer, and when the main beam is contracted, the fiber wavelength becomes shorter. Similarly, when the temperature rises, the fiber wavelength becomes longer, and when the

(a) (b) (c) (d)

Fig. 6. (Color online) On-site fiber layout: (a) grinding and leveling surface, (b) pouring of glue, (c) external protection, and (d) completion of construction.

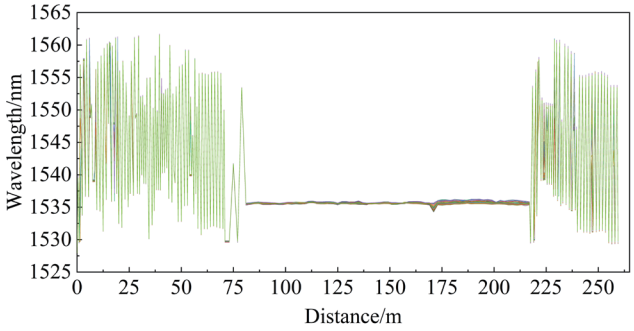

Fig. 7. (Color online) Original wavelength.

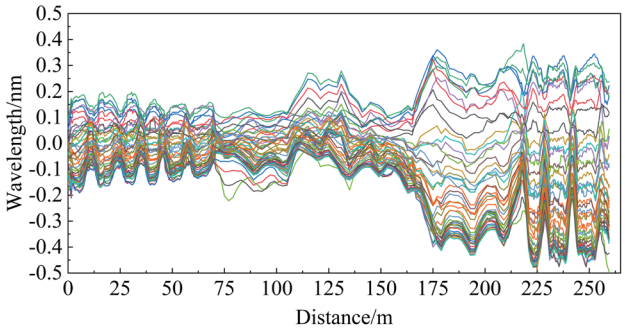

Fig. 8. (Color online) Relative variation of wavelength.

temperature decreases, and the fiber wavelength becomes shorter. In Figs. 7 and 8, 0–71 m corresponds to the lower chord strain measurement fiber, 83–154 m corresponds to the lower chord temperature compensation fiber, 180–217 m corresponds to the upper chord temperature compensation fiber, 217–254 m corresponds to the upper chord strain measurement fiber, and the remaining region comprises redundant segments.

From the measurement results, it was found that in the measured segments, the difference in the wavelength change between the strain measurement section and the temperature compensation section is small, and the temperature is the main factor causing the wavelength change, where the data were measured in the 83–154 m and 180–217 m segments of the lower

chord and the upper chord temperature compensation fiber, and the wavelength change is only affected by temperature. The change in the wavelength of the temperature compensation fiber of the lower chord section is between −0.2 and 0.3 nm, and the temperature change of this section is in the range of −4.4–6.6 °C, as determined using the temperature–wavelength calibration coefficient of 22 °C/nm. The wavelength change of the fiber with temperature compensation of the upper chord section is between −0.4 and 0.35 nm, corresponding to a temperature change of −8.8–7.7 °C. The reason for the different temperature changes in the upper and lower chords is that the upper chord is exposed to sunlight and is more greatly affected by temperature, whereas the lower chord is generally not exposed to sunlight.

To analyze the relative change in the strain of the main beam 24 h after the start of the measurement relative to the start of the measurement, the first measurement result obtained at 11:02 on July 20, 2021 is taken as the reference value and the difference between it and the last measurement result obtained at 11:02 on July 21, 2021 is calculated. After temperature compensation, the relative changes in the strain of the lower and upper chords of the measured section are obtained, as shown in Fig. 9. Figure 9(a) shows the relative change in the strain of the lower chord. The B38–B44 segment of the lower chord on the whole exhibits negative strain, showing a state of pressure, where the B41 node is subjected to the maximum pressure of about −120 με. Figure 9(b) shows the relative change in the upper chord strain, where the first half of the upper chord from the J12# cable to the J15# cable section shows positive strain, indicating a tensile state. The second half shows negative strain, indicating a pressure state. In the area of maximum tensile force near the J13# cable node, the tensile strain is about 98 με, and in the area of maximum pressure near the J15# cable node, the compressive strain is about −30 με. Combined with the on-site construction situation and environmental changes, the reason for this phenomenon is that the bridge deck crane moves towards the cantilever section of the main beam in the span, resulting in the main beam being deflected, whereby the lower chord is compressed and the upper chord is stretched. The test results are consistent with the actual situation.

To analyze the relative change in the strain of the main beam 48 h after the start of the measurement relative to the initial measured value, the first measurement result obtained at 11:02 on July 20, 2021 is taken as the benchmark value, and the last result measured at 11:02 on July 22, 2021 is taken as the base value. After temperature compensation, the relative changes in the strain of the lower and upper chords of the measured section are obtained, as shown in

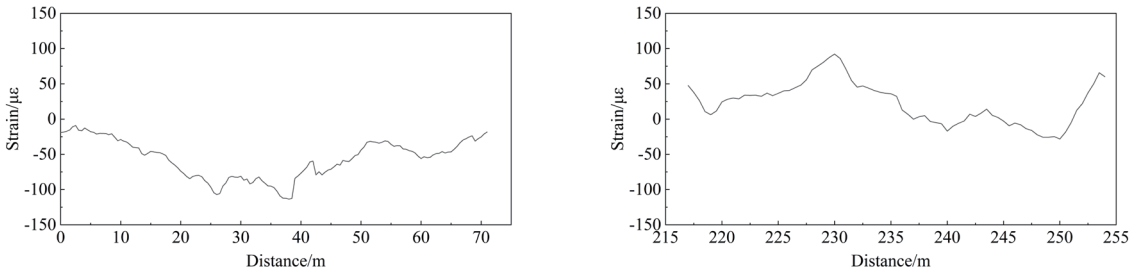

(a) (b)

Fig. 9. Relative variation of strain over 24 h: (a) lower chord and (b) upper chord.

Fig. 10. Figure 10(a) shows the relative change of the lower chord strain. The B38–B44 segment of the lower chord rod on the whole shows positive strain, indicating a tensile state. Figure 10(b) shows the relative change in the upper chord strain. The J12#–J15# cable section of the upper chord on the whole shows negative strain, indicating a pressure state, especially between the J14#–J15# segments, the compression state is obvious, and the compressive strain is about −120 με. Combined with the analysis of the on-site construction situation, during this measurement time period, the tensioning of the J19# cable was being completed, and the cable force was vertically upward and the horizontal inward axial force was applied to the cantilever section of the main beam in the span. This can be expressed as the lower chord being pulled and the upper chord being compressed. The test results are consistent with the actual situation.

The wavelength changes at the strain-dependent weak grating points and temperature-compensated weak grating points at the same position were analyzed, and the wavelength changes of the strain measurement fibers and temperature-compensated optical fibers at the B41 node of the lower chord are plotted in Fig. 11. It can be seen that in the 48 h measurement time, the wavelength changes in the strain measurement fiber and at the weak grating point of the temperature compensation fiber are consistent, indicating that the main factor affecting the wavelength change is the ambient temperature; the wavelength will increase and decrease as the temperature rises and decreases during the day. The strain measurement fiber is smaller than the temperature compensation fiber, and the regularity is not as obvious as in the temperature compensation fiber, because the strain measurement fiber is similarly affected by the ambient temperature, as well as by the change in the strain of the bridge itself.

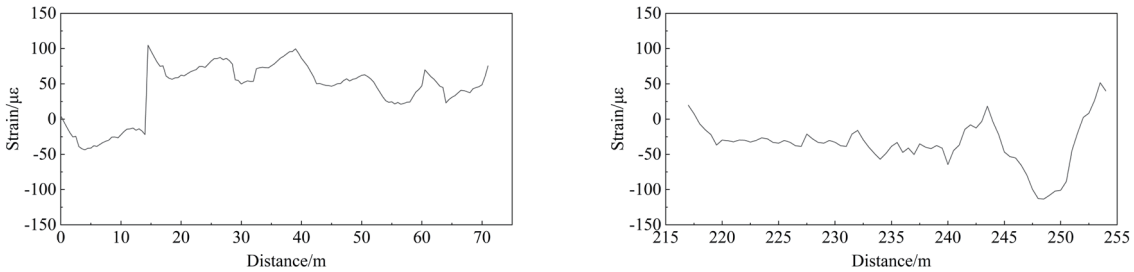

Fig. 10. Relative variation of strain over 48 h: (a) lower chord and (b) upper chord.

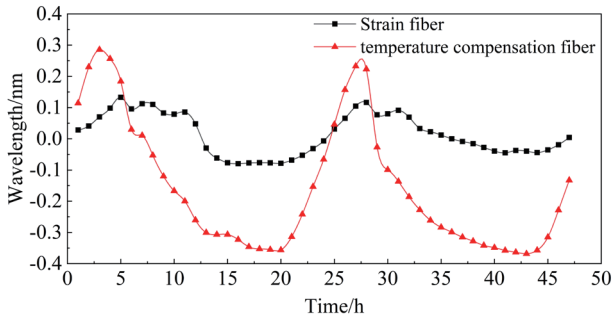

Fig. 11. (Color online) Plots of the relative wavelength at the B41 node strain and temperature gate point.

4. Conclusions

The weak grating array (WFBG) technology was applied to the strain measurement of the main beam during the construction period of the Yangtze River Bridge in Baijusi, Chongqing. The strain measurement fiber and temperature compensating fiber of the weak grating array with intervals of 0.5 and 2 m were laid on the upper and lower chord surfaces of the steel truss main beam, and the strain measurement of the main beam was carried out for 48 h in accordance with the coupling deformation principle of the main beam and the optical fiber. The results show that the weak grating array technology enables the connection of a large number of weak gratings in series on the same optical fiber as needed to achieve distributed monitoring and good engineering application prospect. By the strain monitoring test of the main beam of the cable-stayed bridge using the weak grating array technology, it was found that with the change in the tension and pressure state of the main beam in accordance with the change in the construction state of the bridge, the wavelength of the fiber of the weak grating array also changes correspondingly, which can be used to accurately determine the force state of the main beam. This will have a broad range of application prospects in bridge engineering.

Acknowledgments

This research was funded by the National Development Plan (2021YFF0500900) of China.

References

1 S. Qin and Z. Gao: Engineering-PRC **3** (2017) 787. https://doi.org/10.1016/j.eng.2017.11.001
2 S. Demetrio and S. Salvador: Opt. Express **27** (2019) 38661. https://doi.org/10.1364/OE.379106
3 J. Zhang, X. Xie, and W. Bi: Chin. J. Lasers **40** (2013) 0405006. https://doi.org/CNKI:SUN:JJZZ.0.2013-04-026
4 C. Li, J. Tang, C. Cheng, L. Cai, H. Guo, and M. Yang: Opt. Express **28** (2020) 34309. https://doi.org/10.1364/OE.405536
5 J. Jiang, W. Gan, Y. Hu, S. Li, J. Deng, L. Yue, Y. Yang, Q. Nan, J. Pan, F. Liu, and H. Wang: Measurement **182** (2021) 109744. https://doi.org/10.1016/J.MEASUREMENT.2021.109744
6 J. Jiang, F. Liu, H. Wang, S. Li, W. Gan, and R. Jiang: Measurement **172** (2021) 108892. https://doi.org/10.1016/j.measurement.2020.108892
7 Z. Luo, Y. Zhang, W. Cheng, X. Yang, and S. Zeng: Meas. Sci. Technol. **32** (2021) 055109. https://doi.org/10.1088/1361-6501/abd797
8 Z. Luo, W. Cheng, S. Zeng, and H. He: Appl. Opt. **59** (2020) 9765. https://doi.org/10.1364/AO.402625
9 L. Xin, Z. Li, X. Gui, X. Fu, M. Fan, J. Wang, and H. Wang: Opt. Express **28** (2020) 6794. https://doi.org/10.1364/OE.387317
10 X. Zheng, B. Shi, C. Zhang, Y. Sun, L. Zhang, and H. Han: Measurement **179** (2021) 109510. https://doi.org/10.1016/J.MEASUREMENT.2021.109510
11 Y. Sangyoung, Y. Meadeum, K. Eunho, and Y. Jaesang: Sensors **21** (2021) 3365. https://doi.org/10.3390/S21103365.
12 X. Tan, Y. Bao, Q. Zhang, N. Hani, and G. Chen: Automat. Constr. **124** (2021) 103597. https://doi.org/10.1016/J.AUTCON.2021.103597
13 Y. Zhang, D. Fan, L. Shen, Z. Wu, and J. Qian: Opt. Precis. Eng. **27** (2019) 1481. https://doi.org/10.3788/OPE.20192707.1481